



Proglacial river sediments are a substantial sink of perfluoroalkyl substances released by glacial meltwater

Yunqiao Zhou ¹, Xiaoping Wang ^{1,2}✉, Mengke Chen^{1,2}, Jianjie Fu^{2,3}✉, Tingting Zhu^{1,2}, Chuanfei Wang¹, Ping Gong¹, Lanxiang Wang^{1,2} & Jiao Ren⁴

How climate change will influence the accumulation of pollutants in remote mountainous lakes is poorly understood. Here we collected sediment cores from two glacial lakes (one is small and close to glacier, and the other is large and far from glacier) in the Third Pole and quantified deposition fluxes of perfluoroalkyl substances. The trends of perfluoroalkyl substances fluxes broadly correspond with their historical emissions and phase-out. Besides of emission, glacial meltwater strongly impacts the accumulation of perfluoroalkyl substances in the small lake, while precipitation exhibits great impact on that of the big lake. We then modified the Quantitative Water Air Sediment Interaction model to explore how perfluoroalkyl substances transport along proglacial rivers before entering the big lake and found that river sediments intercept ~13% of perfluoroalkyl substances from glacial meltwater. With climate warming and increased glacial meltwater, proglacial river sediments will play an important role in retaining perfluoroalkyl substances.

¹State Key Laboratory of Tibetan Plateau Earth System, Resources and Environment, Institute of Tibetan Plateau Research, Chinese Academy of Sciences, 100101 Beijing, China. ²University of Chinese Academy of Sciences, 100049 Beijing, China. ³State Key Laboratory of Environmental Chemistry and Ecotoxicology, Research Center for Eco-Environmental Sciences, Chinese Academy of Sciences, 100085 Beijing, China. ⁴Research Institute of Transition of Resource-Based Economics, Shanxi University of Finance and Economics, 030006 Taiyuan, China. ✉email: wangxp@itpcas.ac.cn; jifu@rcees.ac.cn

Now is an efficient scavenger of organic atmospheric pollutants, and the cryosphere is an important contaminant reservoir for this kind of pollution¹. Under global warming, the cryosphere becomes sensitive to climate change;² pollutants, such as persistent organic pollutants (POPs) and mercury, stored in snow/ice, can be released back into the atmosphere and found in freshwater and marine ecosystems^{3,4}.

Perfluoroalkyl substances (PFAS), known as “forever chemicals”, are raising increasing concern, as they already exceed the planetary boundary^{5,6}. To date, PFAS are found ubiquitously worldwide, even in remote polar and alpine regions^{7–9}. Direct long-range atmospheric transport (LRAT) of PFAS, as well as atmospheric transport and degradation of their precursor compounds, are the main PFAS sources in remote regions⁸. In addition, as ionic perfluoroalkyl acids are soluble, they can be effectively scavenged by snow¹⁰. Previous studies have reported high levels of PFAS widely detected in snow and glaciers from remote regions, including parts of the Antarctic^{11–13}, the Arctic^{14,15}, the Tibetan Plateau (TP)¹⁶, and the Alps¹⁷. With climate warming, PFAS deposited in the snow/ice can be secondarily released, transported downwards with glacial runoff, and eventually deposited in the sediment of proglacial lakes¹⁸. However, to date, researches involving PFAS status in proglacial lakes has mainly focused on its release processes^{18,19}, while data about their historical trends are limited and the fate of PFAS along the glacial runoff transport is unclear.

Sediment is the matter that sinks to the bottom of aquatic environments, in this case, the store of pollutants in proglacial rivers and lakes²⁰. On one hand, the sediment cores can be used as effective tools for reconstructing deposition history of pollutants involved^{21,22}. PFAS temporal trends, reconstructed by sediment cores from remote alpine lakes, help to identify the influence of glacier melting during different time periods²². On the other hand, the potential interception of pollutants by river sediments of glacial runoffs has not been evaluated, which may also affect the final accumulation of pollutants in lake sediments²³. Therefore, comprehensive study regarding PFAS transport and loading in proglacial lake basins should be conducted.

The TP is regarded as the “Third Pole” of the Earth, which has a large number of glaciers and lakes^{24,25}. With the shift of PFAS emission sources from North America, Europe and Japan, to China and India, closer to the TP²⁶, the risk of PFAS pollution in these regions has increased, particularly in the southern part of the TP (controlled by the Indian Monsoon)^{10,27}. Additionally, the emissions of PFAS from nearby urban areas and degradation of side-chain fluoropolymers further contribute to this risk²⁸. Previous studies have highlighted that the TP glaciers are an effective reservoir for PFAS^{16,18}. In addition, glaciers in the south part of the TP are retreating rapidly²⁹, which results in more PFAS being released to the lakes fed by glacial meltwater¹⁸.

In this study, we selected two proglacial lakes in the southern TP [the Qiangyong (QY) Lake and the Pumoyong (PM) Lake] (Fig. 1). These two lakes are both influenced by pollution from southern Asia, and exhibit an increasingly warm climate³⁰. However, there are notable differences between the two lake basins. The QY Lake is small and directly fed by glacier meltwater, whereas the PM Lake is big and situated further away from the upper glacier. Our study involved collecting sediment cores from these two lakes and establishing a multi-media fate model for PFAS, with aims to (1) obtain PFAS levels in remote proglacial lakes and reconstruct their deposition records; (2) investigate how climate affects PFAS accumulation; and (3) quantify the role of glacial rivers in intercepting PFAS. This study addresses a gap in understanding pollutant accumulation in the

cryospheric lakes, especially under the complex impact of climate change and basin features.

Results and discussion

Occurrence and historical trends of PFAS in sediment cores.

Thirteen and ten PFAS were detected in the sediment cores of the QY and PM Lake, respectively (Supplementary Tables 1 and 2). The average concentrations of PFAS for the QY sediments (421 pg g^{-1} dry weight, dw) and PM sediments (665 pg g^{-1} dw), as well as the comparisons with other lakes globally, are outlined in Table 1. As expected, PFAS concentrations in sediments from the Tibetan Lakes are lower than that of the Great Lakes ($>4700 \text{ pg g}^{-1}$ dw)^{31,32} and the Chaohu Lake of eastern China ($>1000 \text{ pg g}^{-1}$ dw)³³, where are extensively affected by industrial and human activities. Compared with sediment from the remote alpine lakes in the high Arctic region ($<161 \text{ pg g}^{-1}$ dw)²², PFAS concentrations in sediment from the QY and PM lakes are slightly higher, while comparable to the data from the low Arctic Lake ($44\text{--}1520 \text{ pg g}^{-1}$ dw)²². The relatively low concentration of PFAS in sediment of the Third Pole lakes (QY and PM) supports the notion that the primary sources of PFAS in these lakes are the atmospheric oxidation and deposition of neutral PFAS precursors during LRAT³⁴.

For both QY and PM Lake, perfluorooctanoic acid (PFOA), perfluorooctane sulfonic acid (PFOS), perfluorobutane sulfonic acid (PFBS) and perfluorobutanoic acid (PFBA) were the most consistently detected PFAS (Supplementary Table 3). PFOA and PFOS are considered the end products of the degradation of PFAS precursors^{35–37}, and as such, they are the most ubiquitous PFAS in QY and PM lakes, with the total proportion reaching up to 36% (Supplementary Table 3). Previous researches also reported a higher proportion of PFOA and PFOS in sediment samples, including sediments from the East China Sea³⁸ and Canadian Arctic lakes²². The proportion of PFBS in sediment cores from the two proglacial lakes was found to be relatively high, accounting for ~23% of the total PFAS. Comparable findings have been reported in previous studies of Lake Hazen in the High Arctic²² and Lake Ontario³⁹. This could be partly due to the widespread production of PFBS as an alternative to PFOS³⁹. Notably, the proportions of PFBA in sediment cores are relatively high, at 19% and 16% for the QY and PM lakes, respectively (Supplementary Table 3). Elevated levels of PFBA in glacier snow/ice and meltwater were also found on the Third Pole^{16,18}. As proglacial lakes, particularly the QY Lake, receive a high portion of glacial meltwater, it is likely that the higher PFBA proportions observed in the sediment cores are associated with the glacial meltwater.

The historical trends of PFAS concentrations in sediment cores from QY and PM lakes are displayed in Fig. 2a, b. Considering the potential margin of error in sediment dating, which can be up to ± 5 years per layer, the observed temporal trends (y-axis) are presented in 5-year intervals. The total PFAS concentration generally presents an increasing trend in sediment from the QY Lake during the period of 1958–2009, and the peak value occurred around the early 1980s (Fig. 2a); while the PFAS level in sediment from the PM Lake increased from 1958 to 2004, and was then followed by a decreased trend, with a peak occurring in the middle 1970s and early 2000s (Fig. 2b). This result closely aligns with findings observed in sediment cores obtained from Chaohu Lake in Eastern China³³ and Lake Ontario, Canada³¹. The global emission history of PFAS was presented in Supplementary Fig. 1 based on data reported by previous studies^{40,41}, which indicated that emissions steadily increased from 1970s until the early 2000s, followed by a decrease after the largest PFAS

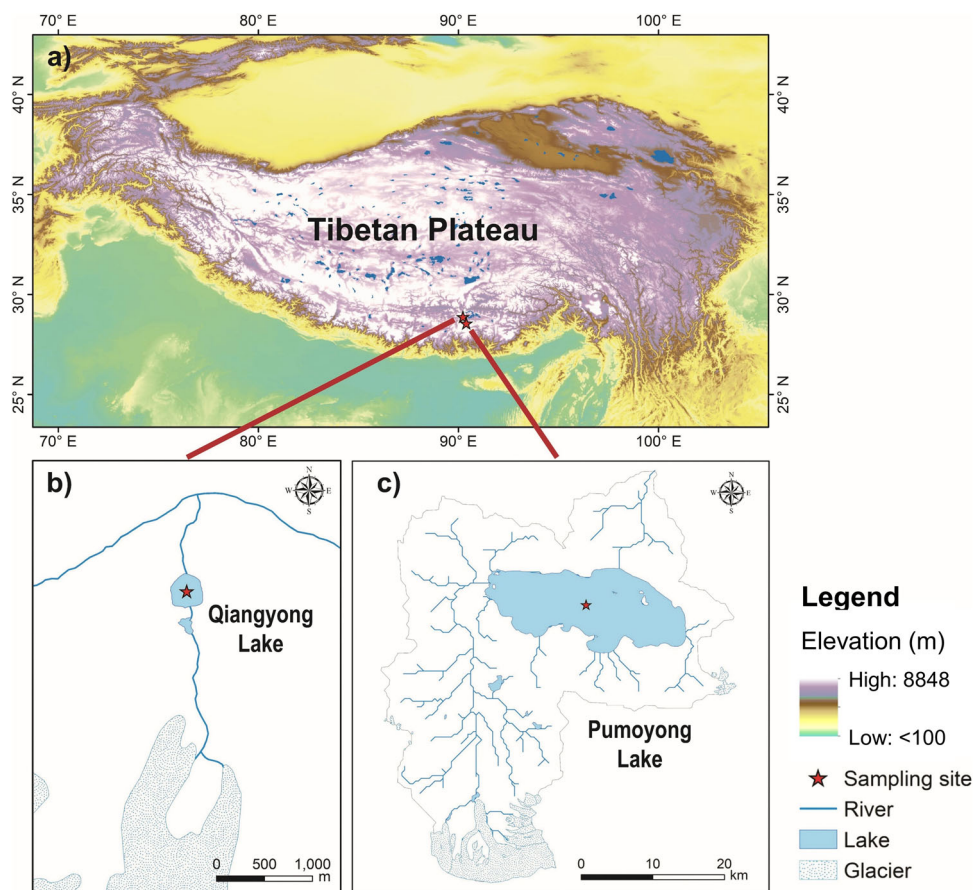


Fig. 1 Spatial distribution of sediment core sampling sites on the Tibetan Plateau. **a** Geographic location of the two studied proglacial lakes, Qiangyong (QY) Lake and Pumoyong (PM) Lake, on the Tibetan Plateau. **b** Sampling site of the sediment core collected in QY Lake. **c** Same as **b** but for PM Lake. The red stars mark the specific sediment core sampling sites. The elevation data on this map is derived from the Digital Elevation Model (DEM) provided by the Geospatial Data Cloud site, Computer Network Information Center, Chinese Academy of Sciences (<http://www.gscloud.cn>).

producer, the 3M company, announced a global phase-out of PFOS in 2002⁴¹. When considering these findings collectively, the transient elevation of PFAS levels in the sediment cores of the TP during the 1970s and early 1980s can be attributed to the substantial increase in global production of perfluorooctylsulfonyl fluoride (POSF)-based products²⁰, alongside the LRAT of PFAS¹⁰.

When analyzing dated ice core samples, it is worth noting that the concentrations of PFBA near the year 1970 were consistently low, often falling below the detection limit, as reported in previous studies^{15,16,19,20}. This suggests minimal or negligible PFBA deposition during that period. The disparities in PFAS records between ice cores and sediment cores can primarily be attributed to inherent characteristics of the sample types. PFAS compounds stored in ice cores tend to be immobile and less prone to migration, whereas short-chain PFBA exhibits the ability to move downward within sediment layers. A field study conducted in Tokyo Bay, Japan, as reported by Ahrens et al. (2009)⁴², demonstrated the downward migration of short-chain PFAS through pore water in sediments. The relatively higher concentration of PFBA observed in the 1970s can be explained by its downward migration via pore water within the sediment layers in Tibetan lakes during that period. Therefore, PFBA and PFBS were removed when calculating the total PFAS (\sum_{11} PFAS) fluxes (Fig. 2c, d).

The variations of PFAS concentrations in sediment cores from these two lakes are broadly similar, likely due to similar atmospheric circulation and the influence of comparable source

regions. However, there are some notable differences between the two lakes, such as a decline in PFAS levels observed in the PM Lake after 2004, which contrasts with the increasing trend observed in the QY Lake after 2000 (Fig. 2a, b). The source regions of PFAS in the TP are generally considered to be Southern and Eastern Asian countries^{23,43,44}. This led us to expect that PFAS concentrations in recent sediments from both QY and PM Lake would increase. However, this expectation was only observed in the sediment of QY Lake (Fig. 2a) and not in PM Lake (Fig. 2b). These findings suggest that factors other than PFAS emissions from industrial sources may also influence the accumulation of PFAS in the proglacial lakes.

Accumulation of PFAS in sediment cores. Compared to the concentration data, the deposition fluxes can reflect the accumulation of pollutants in the sediment cores. Therefore, we calculated the \sum_{11} PFAS deposition fluxes from the two sediment cores. The deposition flux of \sum_{11} PFAS for the QY and the PM lakes reached up to 402 and 865 ng m⁻² y⁻¹, respectively (Supplementary Table 4). These values were similar to that reported for lake sediment cores from the Lake Hazen in the High Arctic²² and deposition fluxes in the PM Lake were about twice than that in the QY Lake. This raised the question why deposition fluxes of PFAS in those remote areas displayed such large variability. When compared to the Arctic, the TP is closer to the source areas, such as south Asian countries^{45,46} and Eastern China⁴¹, thus, the proximity to emission sources likely lead to their high PFAS

Table 1 Comparison of perfluoroalkyl substances (PFAS) concentrations in sediment cores from the Qiangyong (QY) and Pumoyong (PM) Lakes, with those of other lakes.

Analyte	Number of compounds (a + b)	Concentrations (pg g ⁻¹ dw)	Lakes	Site	Characteristics of sampling lakes	Period	Ref.
PFAS	13	208–653 (421)	Lake QY	the Tibetan Plateau	Remote proglacial lake	1958–2009	This study 22
PFAS	11 + 2	356–1067 (665) 6–161	Lake PM Lake Hazen	Canada, high Arctic	Remote proglacial lake	1958–2013 1963–2011	
PFAS	13 + 5	44–1520 <LOD–46600 (8700)	Lake B35 Lake Superior	Canada, low Arctic North American	Remote lake	1952–2009 1880–2011	
PFAS	12 + 2	1100–68300 (10900) <LOD–46500 (4700) 1150–42989	Lake Michigan Lake Huron Lake Ontario	North American North American Niagara Basin	Relatively remote with low population density in watersheds Industrialized region with dense population	1880–2011 1880–2012 1953–2004	31
PFAS	12 + 2	492–3833 591–13083 ~1000–79000	Lake L	Mississauga Basin Rochester Basin Northern Sweden	Influenced by discharge from the Toronto and west end sources Influenced by discharge at the Niagara River and the industry	1952–2005 1954–2003 1968–2009	65
PFAS	13 + 3	480–266 (1881) 280–221 (1378) 210–1750 (1062)	Lake Chaohu	Eastern China	Influenced by a firefighting training facility Influenced by agriculture and urban regions	1952–2006	33

a represents the number of PFAS analyzed in the study that coincide with this study, and b represents the number of other PFAS that differ from this study.

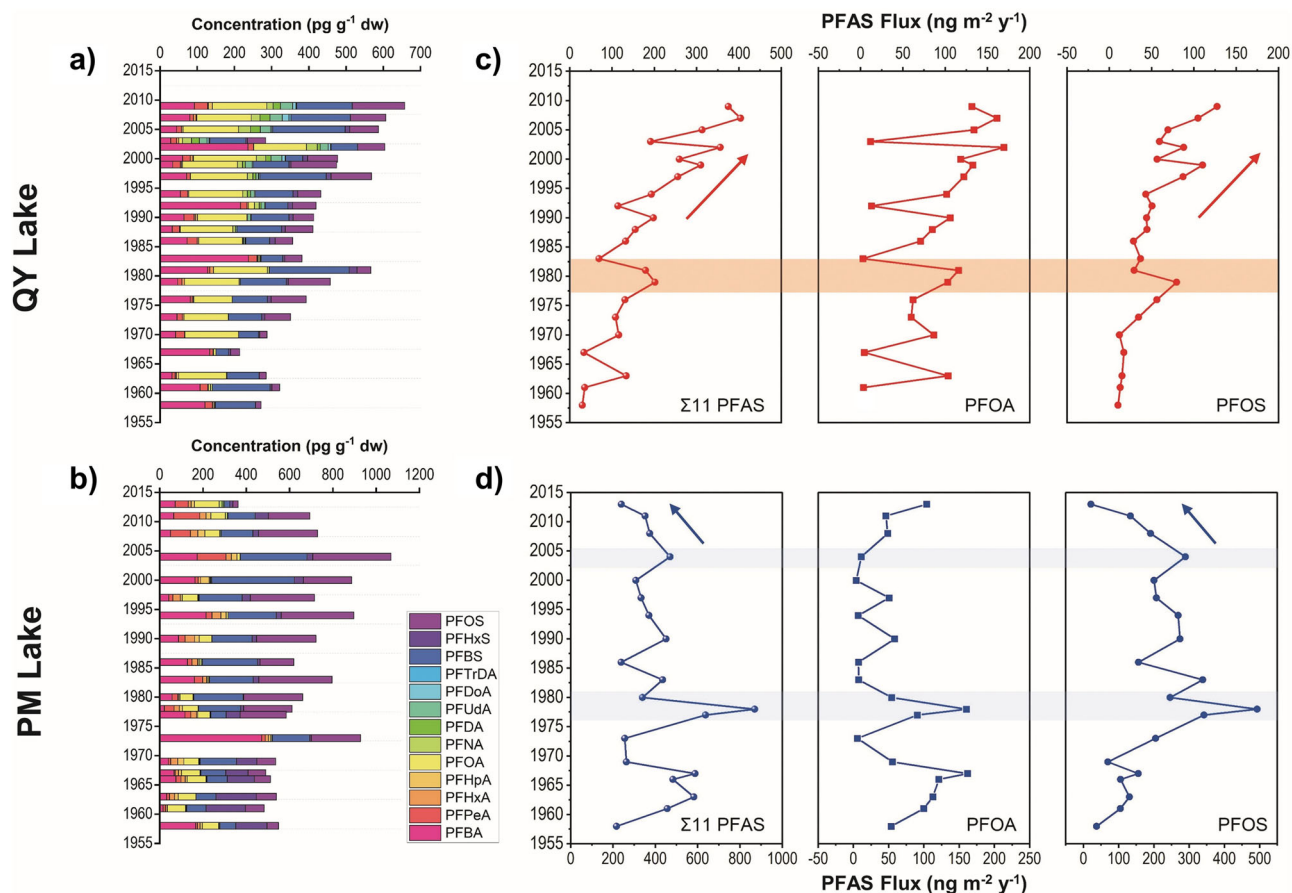


Fig. 2 Concentration and deposition flux of perfluoroalkyl substances (PFAS) in the two sediment cores. Concentration of perfluoroalkyl substances in the sediment core collected from Qiangyong (QY) Lake (a) and Pumoyong (PM) Lake (b). Deposition flux of Σ_{11} PFAS (except for PFBA and PFBS) and the dominant compound (PFOA and PFOS) obtained from the sediment core of QY Lake (c) and PM Lake (d). The date (year) of each sediment core sample is calculated based on ^{210}Pb results using the Constant Rate of Supply (CRS) model, with detailed results listed in Supplementary Tables 14 and 15. Note: The target PFAS congeners include perfluorobutanoic acid (PFBA), perfluoropentanoic acid (PFPeA), perfluorohexanoic acid (PFHxA), perfluoroheptanoic acid (PFHpA), perfluorooctanoic acid (PFOA), perfluorononanoic acid (PFNA), perfluorodecanoic acid (PFDA), perfluoroundecanoic acid (PFUdA), perfluorododecanoic acid (PFDoA) and perfluorotridecanoic acid (PFTTrDA), perfluorobutane sulfonic acid (PFBS), perfluorohexane sulfonic acid (PFHxS) and perfluorooctane sulfonic acid (PFOS).

deposition fluxes. Due to the close positions and similar altitudes, QY and PM lake basins are influenced by similar atmospheric circulation; the difference is that the QY Lake (0.1 km^2) is a small lake directly supplied by glacial meltwater; while PM (290 km^2) is about 2900 times bigger than QY and before the glacial runoffs enter the PM Lake, the glacial rivers pass $\sim 300 \text{ km}$ in total distance. The basin features of PM Lake are more complicated than those for QY Lake - gain more wet deposition and have large area of sediments (including both river and lake sediment).

In order to further clarify the reasons underlying the difference of deposition fluxes, data of PFAS deposition fluxes in the Tibetan glaciers were gathered (Supplementary Table 4). The historical record of PFAS in a glacier from the Mt. Zuoqiupu (also located at the southeast TP)¹⁶ revealed the Σ_{11} PFAS fluxes in snow core was 114 to $358 \text{ ng m}^{-2} \text{ y}^{-1}$, which was lower than that in sediment cores from PM Lake (Supplementary Table 4). Glaciers receive PFAS contaminants solely from the atmosphere; thus, lakes close to glaciers mainly receive PFAS from both atmospheric deposition and meltwater input; while lakes located relatively far from a glacier would receive PFAS via more complicated processes, including atmospheric deposition, meltwater input, and lake basin features which influence the sequestration of PFAS around lake (i.e. organic carbon content

in lake sediments and contact area of water flow from glacier terminal to lake patch).

The historical trends of the Σ_{11} PFAS deposition fluxes and fluxes of dominant PFAS are displayed in Fig. 2c, d. The pattern is broadly similar to what was observed for the temporal trend of PFAS concentrations (Fig. 2a, b). As for the PM Lake, the deposition fluxes of the total PFAS and PFOS increased to the early 2000s, and then decreased after about 2004 (Fig. 2d). In order to clarify the difference between the temporal trend of PFAS deposition fluxes in the QY and PM lakes, analyzing the relationships between PFAS sedimentary deposition fluxes alongside environmental factors will help to reveal the controlling factors that influence the accumulation of PFAS in different lakes.

PFAS accumulation and the influence of sedimentary environment. Climate is closely related to the sedimentary environment of the lakes and Supplementary Fig. 2 illustrates how the deposition fluxes of PFAS relate to climate and geochemical indicators. In the case of the QY Lake, significant positive correlations ($r = 0.612$, $p < 0.01$) were observed between PFAS flux and temperature (Supplementary Fig. 2a), which indicates that glacier meltwater is an important factor affecting PFAS

accumulation in the sediment of the QY Lake. A non-significant correlation was present between PFAS flux of the QY Lake and precipitation and total organic carbon (TOC) (Supplementary Fig. 2b), suggesting that precipitation might play a minor role. In contrast, the PFAS flux in PM Lake did not exhibit statistically significant correlations with temperature (Supplementary Fig. 2g), but instead showed positive correlations ($r = 0.418$, $p < 0.05$) with precipitation (Supplementary Fig. 2h). These findings suggest that warming does not directly increase the accumulation of PFAS in PM Lake, while precipitation can have a great impact, particularly given the large area of the lake ($\sim 290 \text{ km}^2$).

The concentrations of Ti, IC (with main component of CaCO_3) and ratio of Rb/Sr in sediments are commonly used to indicate an input of terrigenous detrital matter, which can reflect the extent of runoff erosion in lake catchment²³. In previous published studies, Ti fluxes had been attributed as an indicator to represent the extent of glacier melting^{23,43} – the higher the flux, the greater the melting would be. As the QY Lake is mainly supplied by glacial meltwater and the debris particles in the sediment core originated from mantle supply in moraines and iron sand, the strong correlations between PFAS flux and Ti flux ($r = 0.562$, $p < 0.05$, Supplementary Fig. 2c), and between PFAS flux and IC ($r = 0.463$, $p < 0.05$, Supplementary Fig. 2d) approved the close association of PFAS accumulation and input of glacial meltwater in the QY Lake, although that between PFAS flux and Rb/Sr ratios is not statistically significant (Supplementary Fig. 2e).

With respect to the PM Lake, correlation efficient between PFAS flux and IC was positive ($r = 0.533$, $p < 0.05$, Supplementary Fig. 2j), while correlation between PFAS flux and Ti Flux ($r = 0.105$, $p > 0.05$, Supplementary Fig. 2i) was not statistically significant, which likely suggests glacial meltwater is not the dominant factor that controls the PFAS accumulation. The correlation analysis (Supplementary Fig. 2a–l) unequivocally establishes that the accumulation of contaminants is not solely dictated by the source and climate (temperature and precipitation), complex features of the basin (glacial runoff) should be linked to the accumulation.

Quantitative estimation of the impact of climate on PFAS accumulation. The method principal component analysis (PCA) followed by multiple linear regression (MLR) has been applied in quantitatively identifying contributions of various environmental progresses to the accumulation of pollutants^{10,27}. Based on the algorithm of dimension-reduction and clustering, it facilitates to obtain the principal components (PCs, representing dominant processes).

As for the QY and PM lakes, PC1 was controlled by Ti flux and IC, thus, it presents the influence of glacial meltwater; PC2 had a large loading for PFAS concentration and TOC, which can be attributed to the sequestration or storage capability of lake; PC3 was heavily weighted by precipitation (Supplementary Table 5). With respect to the PM Lake, similar groups were also classified, with the loading characteristics of Ti flux, TOC, and precipitation, respectively (Supplementary Table 5).

MLR analysis was subsequently conducted with the factor scores and derived the contribution coefficients (B_i) of each PC (see Method section, Supplementary Table 6). In the sediment of QY Lake, 49% of PFAS loading was attributed to glacier meltwater, while TOC absorption was the second dominant process at 39%, and precipitation deposition accounted for 12% of the total contribution. In contrast, in the sediment of PM Lake, glacier melting and TOC absorption contributed only 30% and 19% of PFAS loading, respectively, while precipitation deposition was the dominant process, accounting for 51% of the total contribution. It is interesting to note that the accumulation

mechanisms of PFAS in proglacial lakes can vary depending on the location and basin features.

The individual contributions of each factor to PFAS deposition fluxes of each lake are presented in Fig. 3. In the case of QY Lake, the contribution of glacier melting water increased over time, while lake TOC storage had a relatively constant influence and precipitation deposition had limited effects (Fig. 3a). In the PM Lake, the contribution of glacial melted water peaked in 1980s but subsequently decreased to less than $200 \text{ ng m}^{-2} \text{ y}^{-1}$ (Fig. 3b). As the TOC content continued increase in PM Lake sediment (Supplementary Tables 7 and 8), which may produce more partition media for PFAS in lake, the storage capacity increased over time for hundreds of $\text{ng m}^{-2} \text{ y}^{-1}$ (Fig. 3b). Contribution of precipitation to PM Lake is high but relatively stable after 1980s (Fig. 3b); the reason for the decreased accumulation of PFAS in PM Lake after 2000s can be attributed to that the increased storage caused by increased TOC in lake (tens of $\text{ng m}^{-2} \text{ y}^{-1}$) cannot complement the shortage caused by meltwater ($\sim 60 \text{ ng m}^{-2} \text{ y}^{-1}$).

As PM Lake is larger than QY Lake (290 km^2 vs. 0.1 km^2), it is expected and reasonable that precipitation exhibits a strong impact on the PFAS accumulation in PM Lake. However, the low and decreased glacial melted water contribution in PM Lake is likely the result of the geographical differences between QY and PM Lake (whether proglacial rivers exist), and whether proglacial river sediments can intercept the PFAS released from melted glacier.

River interception effect for PFAS in the proglacial environment. We then modified the Quantitative Water Air Sediment Interaction (QWASI) model by removing the entire air-water interactions (details provided in the Method section) to simulate the transport and fate of PFAS between water and sediment phases of the proglacial rivers (runoff channels) situated in front of PM Lake, with detailed data shown in Fig. 4.

The modeled concentrations of PFAS in each media were first compared with the field-measured values to verify the modified QWASI model's reliability. Our analysis revealed that the total concentrations of PFAS modeled for water and sediment were 667 pg L^{-1} and 328 pg g^{-1} , respectively (Fig. 4). These values were comparable to the field-measured values for water (679 pg L^{-1}) and sediment (363 pg g^{-1}), respectively. The differences observed between the modeled and measured values were less than 10% of the total concentration in each phase (Supplementary Fig. 3). Therefore, the modified QWASI model used in this study was deemed appropriate for assessing the transport of PFAS in the glacial runoff system.

The transport flux analysis (Fig. 4) revealed that within the proglacial environment, the predominant mechanism responsible for PFAS transport into the remote basin is riverine input (441 g y^{-1}), while atmospheric deposition (9.9 g y^{-1}) plays a comparatively minor role. This finding is consistent with the situation in populated areas where the water phase also serves as the primary contributor (67.5%) of PFAS transport⁴⁷. Notably, although the riverine outflow carries 391 g y^{-1} of PFAS downstream (equivalent to 88.7% of the inflow), approximately 57.6 g y^{-1} of PFAS was buried in the riverine sediment, intercepting about 13% of the total PFAS in the water phase (Fig. 4). This is consistent with the findings for Hg in the Himalayan region⁴⁸.

The amount of PFAS intercepted by the river sediment (57.6 g y^{-1}) accounted for about one-third of the accumulation flux (172 g y^{-1}) in the entire PM Lake sediment ($\sim 290 \text{ km}^2$) calculated by the sediment deposition rate. Thus, the interception effect of river sediments in the proglacial environment cannot be ignored, confirming our hypothesis that proglacial river sediments act as important sinks that store PFAS before entering the lake.

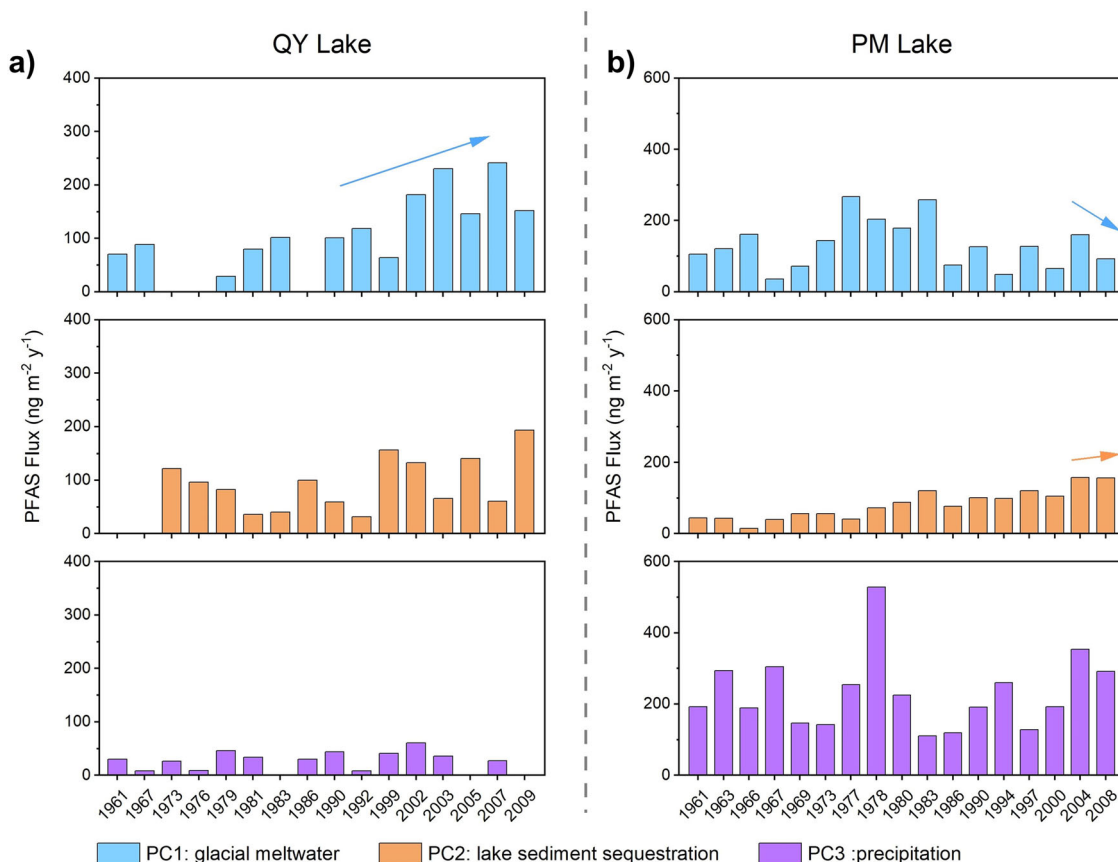


Fig. 3 Contribution of different principal components (PCs) to perfluoroalkyl substances (PFAS) deposition fluxes in the two proglacial lakes. **a** Contribution of glacial meltwater (PC1), lake sediment sequestration (PC2) and precipitation (PC3) to the PFAS deposition fluxes obtained in sediment core from Qiangyong (QY) Lake. **b** Same as **a** but for Pumoyong (PM) Lake. The different PCs are identified by the principal component analysis, with results listed in Supplementary Table 5.

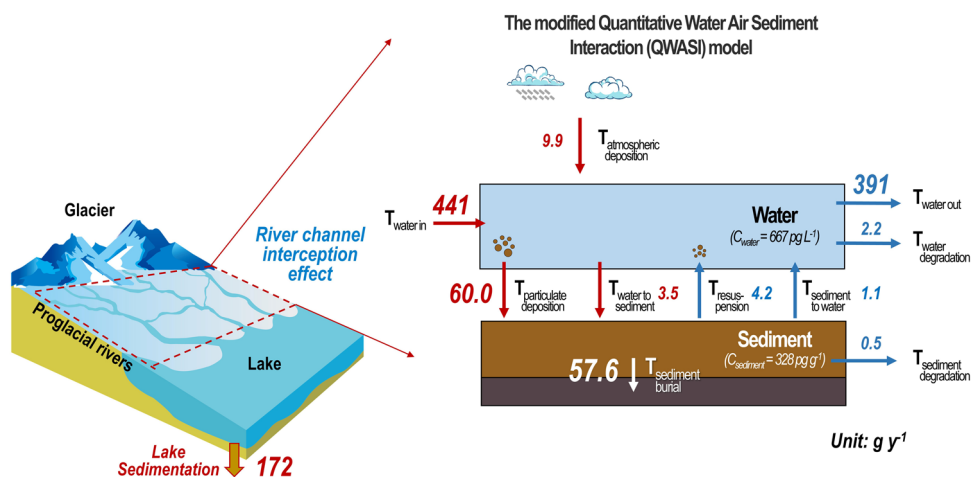


Fig. 4 Transport flux of perfluoroalkyl substances (PFAS) between air, water, and sediment in the proglacial rivers in front of Pumoyong lake. *T* represents the transfer flux and the subscript refers to the specific transport process. The red and blue arrows represent the input and output processes, respectively.

Given that the numerous glacial runoffs typically present between glaciers and lakes on the TP⁴⁹ and they have potential to expand due to climate warming, the storage capacity of PFAS in glacial runoff sediment will be greatly magnified and those PFAS deposited in glacial runoff sediments likely biomagnified and posed risks to benthic phytoplankton taxa (i.e. diatoms,

cryptophytes, and chrysophytes, etc.)^{50,51}, zooplankton taxa (i.e. crustaceans, rotiferans, copepods and nauplii, etc.)^{52,53} and microbial communities⁵⁴ in the proglacial ecosystem. Thus, the sequestration of PFAS in glacial environments, including both glacial river sediments and lake sediments, warrants further close attention.

Conclusions

This study confirms that the major input processes for PFAS accumulation in remote mountainous lakes are transport of melting runoffs and precipitation depositions; both runoff sediments and lake sediments are dominant sinks in lake basin. As glacial runoff increases with climate warming, PFAS deposited in river sediments may increase. PFAS will be subject to biotic and abiotic transformation, creating secondary and tertiary impacts throughout the hydrologic systems of lake basin, posing adverse risks to benthic organisms and creating cascading vulnerabilities to high-elevation aquatic ecosystems. As the cryosphere collapses under climate change, impacts of biogeochemical hazards remobilized from the thawing cryosphere require urgent estimation.

Methods

Study area. The study area focused on the lake basins of QY and PM in the southern TP (Fig. 1), with characteristics detailed in Supplementary Table 9. Climate data, including the annual average temperature and precipitation from a meteorological station close to the two lake basins, was collected and results are shown in Supplementary Fig. 4. The temperature shows an increasing trend, while the precipitation levels display a slight decline, which indicates that climate in both basins is warm and dry^{23,43}.

The QY Lake (~0.1 km²) is a semi-enclosed proglacial lake located between the Himalayan ranges and the Yarlung Zangbo River in the southern TP, where the climate is dominated by the Indian monsoon in summer and the westerlies in winter⁵⁵. The distance between the lake and the terminus of QY glacier is no more than 1 km (Fig. 1), and the hydrological budget of the lake is directly influenced by the intensity of glacier melting, especially in summer, when glacial meltwater is the main water supply²⁶. The hydrological transport characteristics of the QY Lake resemble those of the North and South Polar regions, where PFAS are released into the ocean after release from the glacier¹⁹.

The PM Lake (~290 km²) is a fresh water lake located in the southern of the TP, where the climate is similar to that of the QY Lake. However, the hydrological budget of the PM Lake is more complicated, as it is dominated by >20 major runoffs from the glaciers (with total length about 300 km, Fig. 1) and precipitation deposition⁵⁶. The hydrological transport characteristics of the PM Lake are representative of mountainous glacier regions, characterized by the braided rivers flowing between the glacier and the downstream lake⁵⁷.

Sample collection. In August 2014, we collected two intact sediment cores in the center of the QY Lake (water depth of 18.5 m) and the PM Lake (water depth of 58 m) (Fig. 1), with core depth of 12.5 cm and 10 cm, respectively. The sediment cores were collected using a 9 cm diameter gravity sampler and cut into 0.5 cm per layer along its length, using a stainless-steel cutter in the field. The 0–1 cm sample of the QY core was not quantified for PFAS due to insufficient sample weight (<2 g dry weight), resulting in 23 samples for the QY core and 20 samples for the PM core (Supplementary Tables 1,2). Each sample was lyophilized, ground and stored at –20 °C until analysis. Dry and wet weight, water content, density, porosity, inorganic carbon (IC) and TOC were determined for all samples of the two sediment cores, as seen in Supplementary Tables 7,8. The concentration of trace metals (i.e. Hg, black carbon and Ti) in these two sediment cores was previously reported^{23,43}.

PFAS extraction and analysis. PFAS in sediment were extracted using methanol, with minor modifications²². In brief, approximately 2 g dried sediment core sample spiked with 2000 pg of

recovery standard mix (Supplementary Table 10) was weighed into a 50 mL polypropylene centrifuge tube. Following the addition of 10 mL of methanol, the sample was shaken for two minutes to mix evenly, sonicated at 60 °C for 30 min and centrifuged at 6000 rpm for 15 mins. The supernatant was then transferred to another tube. This process was performed in triplicate. The supernatants were then combined (about 30 mL) and concentrated to 1–2 mL using nitrogen gas, and then diluted with 50 mL of milli-Q water. The dilution was then loaded onto a preconditioned Waters Oasis WAX cartridge (150 mg, 6 cm³), as reported previously¹⁸.

PFAS analysis was conducted using a DGLC-HPLC (UltiMate™ 3000, ThermoFisher Scientific, USA) and a triple quadrupole mass spectrometer (TSQ Quantiva, ThermoFisher Scientific, USA), as reported previously^{58,59} and described in Supplementary Note 1. Quantification was performed using response factors calculated and applied to a 7-point calibration curve, ranging from 0 to 20 ppb for individual analytes. The target analytes, including C4–C13 perfluorocarboxylic acids (PFCAs) and C4, C6 and C8 perfluoroalkanesulfonic acids (PFASAs), are listed in Supplementary Table 11.

Quality assurance and controls. All analytical procedures were monitored using strict quality assurance/control measures. Experimental blanks were conducted for each batch of 10 samples ($n = 5$), to check for possible laboratory contamination, and results are given in Supplementary Table 12. The limit of detection (LOD) was determined at the signal-to-noise (S/N) ratio of 3 for each compound, which ranged from 2.0 to 15.0 pg g⁻¹ dw, and displayed in Supplementary Table 12. Mean recoveries in this study ranged between 42% and 70% for the recovery mix (Supplementary Table 13). All results were recovery corrected.

Sediment core dating and flux calculation. The date and sedimentation rates were calculated based on ²¹⁰Pb results using the Constant Rate of Supply (CRS) model⁶⁰, and the peak of ¹³⁷Cs was used as the time mark for comparison. The activities of ²¹⁰Pb, ¹³⁷Cs and ²²⁶Ra in sediment cores were determined by a high-purity germanium detector (OTEC GWL), and excess ²¹⁰Pb (²¹⁰Pb_{exc}) was obtained by subtracting ²²⁶Ra from ²¹⁰Pb. The absolute efficiency of the detector was tested using sediment samples of known activity and calibration sources. The ¹³⁷Cs activity versus depth in sediment cores from the QY Lake and the PM Lake peaked at 12–12.5 cm and 9–9.5 cm (Supplementary Figs. 5,6), respectively, which recorded the maximum 1963 fallout from the atmospheric testing of nuclear weapons⁶¹. On the other hand, ²¹⁰Pb_{exc} calculation of the CRS model estimates the year at 12.5 cm to be 1958 in the sediment core from the QY Lake, and placed 1958 at 10.0 cm of the PM Lake sediment core (Supplementary Tables 14 and 15). The ¹³⁷Cs and CRS results of sediment cores were seen to have good consistency, which indicates that the chronological sequence is relatively accurate (Supplementary Figs. 5, 6). As a result, due to the absence of the surface two layers (0–1 cm), the QY core represents data spanning from 1958 to 2009, while the PM core includes data ranging from 1958 to 2013 (close to the sampling time of 2014). This provided us with the opportunity to compare the PFAS accumulation of the TP in different climate patterns (dry vs. wet), over half a century (from 1958 to 2013).

The sedimentary fluxes were calculated using the following equations:

$$F_{\text{sed}} = C_{\text{sed}} \times R_{\text{sed}} \times 10 \quad (1)$$

where F_{sed} (ng m⁻² y⁻¹) is the sedimentary fluxes of PFAS; C_{sed} (pg g⁻¹ dw) is the concentration of PFAS in sediment cores; R_{sed}

($\text{g cm}^{-2} \text{y}^{-1}$) is the sedimentary rate. The sediment rates were presented in Supplementary Tables 14, 15.

Principal component and multiple linear regression analysis.

Principal component analysis combined with multiple linear regression analysis (PCA-MLR) was used to apportion different sources of organic pollutants in the environment^{10,27}. PCA is based on varimax rotation and retain principal components (PCs) whose eigenvalues were the top three, the purpose of which is to sort out the major factors that influence the levels of contaminants (Supplementary Fig. 7). The goal of MLR was to quantify the contribution of the different PCs. In brief, factor scores of each PCs obtained from the PCA were regressed against the standard normalized deviate (Z-score)²⁴ and used as independent variables.

$$Z = (X - \mu) / \sigma \quad (2)$$

where Z is the Z-score, X is the data point, μ is the mean of the dataset, and σ is the standard deviation of the dataset.

The MLR was run with the chemical fluxes/concentrations (using PFAS fluxes of sediment cores in this study) as the dependent variables, the details of which can be found in previously published research⁶². The mean percent contribution of each major factor was calculated based on the coefficients (B_i) of the factor scores (determined with a stipulated minimum 95% confidence limit):

$$R_i = \left(\frac{B_i}{\sum_1^n B_n} \right) \times 100\% \quad (3)$$

where R_i (%) is the average contribution of the major factor i , B_i is the normalization factor of the major factor i .

The contribution of each factor i to the PFAS fluxes in each sediment samples (presented different year) involves four main steps, with workflow of calculation shown in Supplementary Fig. 8.

Step 1: Conducted a PCA analysis of selected parameters to obtain PC1, PC2 and PC3, and define the meaning of each PC.

Step 2: Obtain the factor score of each PCs for every sample (dated for different year).

Step 3: Perform a Multiple linear regression (MLR) analysis with the factor scores of PC1, PC2 and PC3 as independent variable and \sum_{11} PFAS flux as the dependent variable to calculate the coefficients (B_i) for each PC.

Step 4: Utilize the obtained values in the following equations to derive the results:

$$F_i = \text{mean } F_{\text{sed}} \times \left(\frac{B_i}{B_i} \right) + B_i \sigma_{F_{\text{sed}}} FS_i \quad (4)$$

where F_i ($\text{ng m}^{-2} \text{y}^{-1}$) refers to the contribution of major factor i to PFAS deposition flux in the sediment core, $\text{mean } F_{\text{sed}}$ denotes the average value of PFAS deposition flux in the sediment core, $\sigma_{F_{\text{sed}}}$ ($\text{ng m}^{-2} \text{y}^{-1}$) is the standard deviation of PFAS deposition flux, and FS_i represents the factor score of major factor i .

Model development and multimedia modeling. To investigate the transport fate of PFAS in the glacial rivers, a modified Quantitative Water Air Sediment Interaction (QWASI) model was used with local parameters^{47,63,64}. The concentrations of all target PFAS in water and sediment and their migration fluxes between these two phrases are simulated. Briefly, the modified QWASI model is based on mass conservation (assuming the water and sediment is well-mixed) by means of defining a series of Z values (aivalent capacity, dimensionless) and D values (transfer parameters, $\text{m}^3 \text{h}^{-1}$), using “aivalence” (A , mol m^{-3}) as the equilibrium criterion to establish a mass balance equation

for the water and sediment phases under state conditions. Of note, the aivalence capacity in water (Z_W) is defined as “1” and A (mol m^{-3}) values represent the aivalence values which could be converted to the phase concentrations (C , pg L^{-1} in water or pg g^{-1} in sediment). The mass conservation equations in the modified QWASI are presented below:

Water phase equation:

$$T_{\text{water in}} + T_{\text{atmospheric deposition}} + T_{\text{resuspension}} + T_{\text{sediment to water}} = T_{\text{particulate deposition}} + T_{\text{water to sediment}} + T_{\text{water out}} + T_{\text{water degradation}} \quad (5)$$

$$(\text{in detail}) E_w + E_A + E_S \times (D_R + D_{SW}) = A_W \times (D_D + D_{WS} + D_O + D_{WU}) \quad (6)$$

Sediment phase equation:

$$T_{\text{particulate deposition}} + T_{\text{water to sediment}} = T_{\text{resuspension}} + T_{\text{sediment to water}} + T_{\text{sediment burial}} + T_{\text{sediment degradation}} \quad (7)$$

$$(\text{in detail}) A_W \times (D_D + D_{WS}) = A_S \times (D_R + D_{SW} + D_B + D_{SU}) \quad (8)$$

where T represents the transfer process, and the subscript refers to the name of the specific process. W refers to water, S refers to Sediment. E_W and E_A are the “input” into the water (g y^{-1}) and the atmospheric deposition (g y^{-1}), respectively, which is calculated by the corresponding mass flux and concentrations. D ($\text{m}^3 \text{h}^{-1}$) is the transfer parameter, D_R is the sediment resuspension, D_{SW} is the sediment-water diffusion, D_D is the suspended particles deposition, D_{WS} is the water-sediment diffusion, D_O is the water outflow, D_{WU} is the degradation of PFAS in water, D_B is the sediment burial, D_{SU} is the degradation of PFAS in sediment. The calculations and parameters for determining the parameter values are described in Supplementary Tables 16 and 17.

The model incorporates 24 parameters that comprise environmental, physical, chemical, and kinetic factors, which have been obtained from a variety of sources such as literature reviews, laboratory experiments, and calculations. Each parameter, along with its symbol, description, value, and source, is listed in Supplementary Tables 18 and 19. The model’s sensitivity was evaluated using the method outlined in Supplementary Note 2 and depicted in Supplementary Fig. 9.

Data availability

All data used to generate charts and graphs are available in the supplementary information of this paper, also published in the National Tibetan Plateau/Third Pole Environment Data Center (<https://doi.org/10.11888/Cryos.tpc.300893>), and available on request to the corresponding author.

Received: 2 June 2023; Accepted: 15 January 2024;

Published online: 06 February 2024

References

- Grannas, A. M. et al. The role of the global cryosphere in the fate of organic contaminants. *Atmos. Chem. Phys.* **13**, 3271–3305 (2013).
- Bourbonnais, A. et al. Global change on the Blue Planet. *Commun. Earth Environ.* **2**, 163 (2021).
- Hung, H. et al. Climate change influence on the levels and trends of persistent organic pollutants (POPs) and chemicals of emerging Arctic concern (CEACs) in the Arctic physical environment—a review. *Environ. Sci. Process. Impacts* **24**, 1577–1615 (2022).

4. Chai, L., Zhou, Y. & Wang, X. Impact of global warming on regional cycling of mercury and persistent organic pollutants on the Tibetan Plateau: current progress and future prospects. *Environ. Sci. Process. Impacts* **24**, 1616–1630 (2022).
5. Cousins, I. T., Johansson, J. H., Salter, M. E., Sha, B. & Scheringer, M. Outside the safe operating space of a new planetary boundary for per- and polyfluoroalkyl substances (PFAS). *Environ. Sci. Technol.* **56**, 11172–11179 (2022).
6. Evich, M. G. et al. Per- and polyfluoroalkyl substances in the environment. *Science* **375**, eabg9065 (2022).
7. Nash, S. B. et al. Perfluorinated compounds in the Antarctic region: ocean circulation provides prolonged protection from distant sources. *Environ. Pollut.* **158**, 2985–2991 (2010).
8. Benskin, J. P., Phillips, V. S. T., Louis, V. L. & Martin, J. W. Source elucidation of perfluorinated carboxylic acids in remote alpine lake sediment cores. *Environ. Sci. Technol.* **45**, 7188–7194 (2011).
9. Myers, A. L. et al. Fate, distribution, and contrasting temporal trends of perfluoroalkyl substances (PFASs) in Lake Ontario, Canada. *Environ. Int.* **44**, 92–99 (2012).
10. Wang, X., Chen, M., Gong, P. & Wang, C. Perfluorinated alkyl substances in snow as an atmospheric tracer for tracking the interactions between westerly winds and the Indian Monsoon over western China. *Environ. Int.* **124**, 294–301 (2019).
11. Wang, Z. et al. Neutral poly/per-fluoroalkyl substances in air from the Atlantic to the Southern Ocean and in Antarctic snow. *Environ. Sci. Technol.* **49**, 7770–7775 (2015).
12. Casal, P. et al. Role of snow deposition of perfluoroalkylated substances at coastal Livingston Island (maritime Antarctica). *Commun. Earth Environ.* **51**, 8460–8470 (2017).
13. Xie, Z. et al. Occurrence of legacy and emerging organic contaminants in snow at Dome C in the Antarctic. *Sci. Total Environ.* **741**, 140200 (2020).
14. MacInnis, J. J. et al. Emerging investigator series: a 14-year depositional ice record of perfluoroalkyl substances in the High Arctic. *Environ. Sci. Process. Impacts* **19**, 22–30 (2017).
15. Pickard, H. M. et al. Continuous non-marine inputs of per- and polyfluoroalkyl substances to the High Arctic: a multi-decadal temporal record. *Atmos. Chem. Phys.* **18**, 5045–5058 (2018).
16. Wang, X. et al. Accumulation of perfluoroalkyl compounds in Tibetan mountain snow: temporal patterns from 1980 to 2010. *Environ. Sci. Technol.* **48**, 173–181 (2014).
17. Kirchgeorg, T. et al. Temporal variations of perfluoroalkyl substances and polybrominated diphenyl ethers in alpine snow. *Environ. Pollut.* **178**, 367–374 (2013).
18. Chen, M. et al. Release of perfluoroalkyl substances from melting glacier of the Tibetan Plateau: Insights into the impact of global warming on the cycling of emerging pollutants. *J. Geophys. Res. Atmos.* **124**, 7442–7456 (2019).
19. Kwok, K. Y. et al. Transport of perfluoroalkyl substances (PFAS) from an arctic glacier to downstream locations: implications for sources. *Sci. Total Environ.* **447**, 46–55 (2013).
20. Prevedouros, K., Cousins, I. T., Buck, R. C. & Korzeniowski, S. H. Sources fate and transport of perfluorocarboxylates. *Environ. Sci. Technol.* **40**, 32–44 (2006).
21. Hites, R. A., Laflamme, R. E. & Farrington, J. W. Sedimentary polycyclic aromatic hydrocarbons: the historical record. *Science* **198**, 829–831 (1977).
22. MacInnis, J. J., Lehnher, I., Muir, D. C., Quinlan, R. & De Silva, A. O. Characterization of perfluoroalkyl substances in sediment cores from High and Low Arctic lakes in Canada. *Sci. Total Environ.* **666**, 414–422 (2019).
23. Lin, H. et al. The influence of climate change on the accumulation of polycyclic aromatic hydrocarbons, black carbon and mercury in a shrinking remote lake of the southern Tibetan Plateau. *Sci. Total Environ.* **601**, 1814–1823 (2017).
24. Yao, T. et al. Different glacier status with atmospheric circulations in Tibetan Plateau and surroundings. *Nat. Clim. Change* **2**, 663–667 (2012).
25. Ren, J., Wang, X., Wang, C., Gong, P. & Yao, T. Atmospheric processes of organic pollutants over a remote lake on the central Tibetan Plateau: implications for regional cycling. *Atmos. Chem. Phys.* **17**, 1401–1415 (2017).
26. Li, J., Xu, B., Lin, S. & Gao, S. Glacier and climate changes over the past millennium recorded by proglacial sediment sequence from Qiangyong Lake, southern Tibetan Plateau. *J. Earth Syst. Environ.* **33**, 402–411 (2011).
27. Liu, X. et al. Forest filter effect versus cold trapping effect on the altitudinal distribution of PCBs: a case study of Mt. Gongga, Eastern Tibetan Plateau. *Environ. Sci. Technol.* **48**, 14377–14385 (2014).
28. Buck, R. C. et al. Perfluoroalkyl and polyfluoroalkyl substances in the environment: terminology, classification, and origins. *Integr. Environ. Assess. Manag.* **7**, 513–541 (2011).
29. Compagno, L., Huss, M., Zekollari, H., Miles, E. S. & Farinotti, D. Future growth and decline of high mountain Asia’s ice-dammed lakes and associated risk. *Commun. Earth Environ.* **3**, 191 (2022).
30. Zhang, X., Xu, B., Xie, Y., Li, J. & Li, Y. Continuous mass loss acceleration of Qiangyong Glacier, southern Tibetan plateau, since the mid–1880s inferred from glaciolacustrine sediments. *Quat. Sci. Rev.* **301**, 107937 (2023).
31. Yeung, L. W. et al. Perfluoroalkyl substances and extractable organic fluorine in surface sediments and cores from Lake Ontario. *Environ. Int.* **59**, 389–397 (2013).
32. Codling, G. et al. Current and historical concentrations of poly and perfluorinated compounds in sediments of the northern Great Lakes–Superior, Huron, and Michigan. *Environ. Pollut.* **236**, 373–381 (2018).
33. Qi, Y. et al. Spatial distribution and historical deposition behaviors of perfluoroalkyl substances (PFASs) in sediments of Lake Chaohu, a shallow eutrophic lake in Eastern China. *Ecol. Indic.* **57**, 1–10 (2015).
34. Wang, X., Schuster, J., Jones, K. C. & Gong, P. Occurrence and spatial distribution of neutral perfluoroalkyl substances and cyclic volatile methylsiloxanes in the atmosphere of the Tibetan Plateau. *Atmos. Chem. Phys.* **18**, 8745–8755 (2018).
35. Armitage, J. M. et al. Modeling the global fate and transport of perfluorooctane sulfonate (PFOS) and precursor compounds in relation to temporal trends in wildlife exposure. *Environ. Sci. Technol.* **43**, 9274–9280 (2009).
36. Jiang, W., Zhang, Y., Yang, L., Chu, X. & Zhu, L. Perfluoroalkyl acids (PFAAs) with isomer analysis in the commercial PFOS and PFOA products in China. *Chemosphere* **127**, 180–187 (2015).
37. Ye, F., Zushi, Y. & Masunaga, S. Survey of perfluoroalkyl acids (PFAAs) and their precursors present in Japanese consumer products. *Chemosphere* **127**, 262–268 (2015).
38. Wang, Q.-W., Yang, G.-P., Zhang, Z.-M. & Jian, S. Perfluoroalkyl acids in surface sediments of the East China Sea. *Environ. Pollut.* **231**, 59–67 (2017).
39. Christensen, E. R., Zhang, R., Codling, G., Giesy, J. P. & Li, A. Poly- and perfluoroalkyl compounds in sediments of the Laurentian Great Lakes: loadings, temporal trends, and sources determined by positive matrix factorization. *Environ. Pollut.* **255**, 113166 (2019).
40. Schenker, U. et al. Contribution of volatile precursor substances to the flux of perfluorooctanoate to the Arctic. *Environ. Sci. Technol.* **42**, 3710–3716 (2008).
41. Wang, Z., Cousins, I. T., Scheringer, M., Buck, R. C. & Hungerbühler, K. Global emission inventories for C4–C14 perfluoroalkyl carboxylic acid (PFCA) homologues from 1951 to 2030, Part I: production and emissions from quantifiable sources. *Environ. Int.* **70**, 62–75 (2014).
42. Ahrens, L. et al. Partitioning behavior of per- and polyfluoroalkyl compounds between pore water and sediment in two sediment cores from Tokyo Bay, Japan. *Environ. Sci. Technol.* **43**, 6969–6975 (2009).
43. Zhu, T. et al. Accumulation of pollutants in proglacial lake sediments: impacts of glacial meltwater and anthropogenic activities. *Environ. Sci. Technol.* **54**, 7901–7910 (2020).
44. Kang, S. et al. Atmospheric mercury depositional chronology reconstructed from lake sediments and ice core in the Himalayas and Tibetan Plateau. *Environ. Sci. Technol.* **50**, 2859–2869 (2016).
45. Wang, X., Xu, B., Kang, S., Cong, Z. & Yao, T. The historical residue trends of DDT, hexachlorocyclohexanes and polycyclic aromatic hydrocarbons in an ice core from Mt. Everest, central Himalayas, China. *Atmos. Environ.* **42**, 6699–6709 (2008).
46. Sheng, J. et al. Monsoon-driven transport of organochlorine pesticides and polychlorinated biphenyls to the Tibetan Plateau: three year atmospheric monitoring study. *Environ. Sci. Technol.* **47**, 3199–3208 (2013).
47. Zhou, Y. et al. Optimizing the fugacity model to select appropriate remediation pathways for perfluoroalkyl substances (PFASs) in a lake. *J. Hazard. Mater.* **438**, 129558 (2022).
48. Sun, X. et al. Melting Himalayas and mercury export: results of continuous observations from the Rongbuk Glacier on Mt. Everest and future insights. *Water Res.* **218**, 118474 (2022).
49. Zhang, F., Zeng, C., Zhang, Q. & Yao, T. Securing water quality of the Asian Water Tower. *Nat. Rev. Earth Environ.* **3**, 611–612 (2022).
50. Lindborg, T. et al. Biogeochemical data from terrestrial and aquatic ecosystems in a periglacial catchment, West Greenland. *Earth Syst. Sci. Data* **8**, 439–459 (2016).
51. Casal, P. et al. Accumulation of perfluoroalkylated substances in oceanic plankton. *Environ. Sci. Technol.* **51**, 2766–2775 (2017).
52. Jeppesen, E. et al. Differences in food web structure and composition between new and nearby older lakes in West Greenland suggest succession trajectories driven by glacier retreat. *Hydrobiologia* **850**, 4745–4761 (2023).
53. Abramova, E. et al. Structure of freshwater zooplankton communities from tundra waterbodies in the Lena River Delta, Russian Arctic, with a discussion on new records of glacial relict copepods. *Polar Biol.* **40**, 1629–1643 (2017).
54. Faucher, B. et al. Glacial lake outburst floods enhance benthic microbial productivity in perennially ice-covered Lake Untersee (East Antarctica). *Environ. Sci. Technol.* **2**, 211 (2021).

55. Yao, T. et al. A review of climatic controls on $\delta^{18}\text{O}$ in precipitation over the Tibetan Plateau: observations and simulations. *Rev. Geophys.* **51**, 525–548 (2013).
56. Wang, J., Zhu, L., Ju, J., Xia, M. & Wang, Y. Environmental change reflected by a comparative proxy study among multiple cores from Pumoyum Co, Tibet in the last 200 years. *J. Lake Sci.* **21**, 819–826 (2009).
57. Lai, R. et al. Streamline-based method for reconstruction of complex braided river bathymetry. *J. Hydrol. Eng.* **26**, 04021012 (2021).
58. Gao, K., Gao, Y., Li, Y., Fu, J. & Zhang, A. A rapid and fully automatic method for the accurate determination of a wide carbon-chain range of per- and polyfluoroalkyl substances (C4–C18) in human serum. *J. Chromatogr. A* **1471**, 1–10 (2016).
59. Gao, K. et al. Prenatal exposure to per- and polyfluoroalkyl substances (PFASs) and association between the placental transfer efficiencies and dissociation constant of serum proteins–PFAS complexes. *Environ. Sci. Technol.* **53**, 6529–6538 (2019).
60. Oldfield, F., Appleby, P. & Battarbee, R. Alternative ^{210}Pb dating: results from the New Guinea Highlands and Lough Erne. *Nature* **271**, 339–342 (1978).
61. Garcia-Orellana, J. et al. Atmospheric fluxes of ^{210}Pb to the western Mediterranean Sea and the Saharan dust influence. *J. Geophys. Res. Atmos.* **111**, D15305 (2006).
62. Larsen, R. K. & Baker, J.E. Source apportionment of polycyclic aromatic hydrocarbons in the urban atmosphere: a comparison of three methods. *Environ. Sci. Technol.* **37**, 1873–1881 (2003).
63. Mackay, D., Hughes, L., Powell, D. E. & Kim, J. An updated Quantitative Water Air Sediment Interaction (QWASI) model for evaluating chemical fate and input parameter sensitivities in aquatic systems: application to D5 (decamethylcyclopentasiloxane) and PCB-180 in two lakes. *Chemosphere* **111**, 359–365 (2014).
64. Mackay, D. & Diamond, M. Application of the QWASI (Quantitative Water Air Sediment Interaction) fugacity model to the dynamics of organic and inorganic chemicals in lakes. *Chemosphere* **18**, 1343–1365 (1989).
65. Mussabek, D., Ahrens, L., Persson, K. M. & Berndtsson, R. Temporal trends and sediment–water partitioning of per- and polyfluoroalkyl substances (PFAS) in lake sediment. *Chemosphere* **227**, 624–629 (2019).

Acknowledgements

This study was funded by the National Natural Science Foundation of China [grant number 41925032 and 42107438], the Second Tibetan Plateau Scientific Expedition and Research Program (STEP) [grant number 2019QZKK0605], and the China Postdoctoral Science Foundation [grant number 2020M680696 and 2023T160659].

Author contributions

Y.Z. analyzed the data and drafted the paper; X.W. conceived the idea and study design; M.C. collected and analyzed the data; J.F. contributed to the analytical tools and methodology; T.Z., C.W., P.G., L.W., and J.R. revised the paper. All authors contributed to the interpretation.

Competing interests

The authors declare no competing interests.

Additional information

Supplementary information The online version contains supplementary material available at <https://doi.org/10.1038/s43247-024-01223-y>.

Correspondence and requests for materials should be addressed to Xiaoping Wang or Jianjie Fu.

Peer review information *Communications Earth & Environment* thanks Jingjie Zhang and the other, anonymous, reviewer(s) for their contribution to the peer review of this work. Primary Handling Editors: Clare Davis. A peer review file is available.

Reprints and permission information is available at <http://www.nature.com/reprints>

Publisher's note Springer Nature remains neutral with regard to jurisdictional claims in published maps and institutional affiliations.



Open Access This article is licensed under a Creative Commons Attribution 4.0 International License, which permits use, sharing, adaptation, distribution and reproduction in any medium or format, as long as you give appropriate credit to the original author(s) and the source, provide a link to the Creative Commons licence, and indicate if changes were made. The images or other third party material in this article are included in the article's Creative Commons licence, unless indicated otherwise in a credit line to the material. If material is not included in the article's Creative Commons licence and your intended use is not permitted by statutory regulation or exceeds the permitted use, you will need to obtain permission directly from the copyright holder. To view a copy of this licence, visit <http://creativecommons.org/licenses/by/4.0/>.

© The Author(s) 2024